A multi-state memory device based on the unidirectional spin Hall magnetoresistance

Can Onur Avci, Maxwell Mann, Aik Jun Tan, Pietro Gambardella, and Geoffrey S. D. Beach

Citation: Appl. Phys. Lett. **110**, 203506 (2017); doi: 10.1063/1.4983784
View online: http://dx.doi.org/10.1063/1.4983784
View Table of Contents: http://aip.scitation.org/toc/apl/110/20
Published by the American Institute of Physics

A multi-state memory device based on the unidirectional spin Hall magnetoresistance

Can Onur Avci,[1,a)] Maxwell Mann,[1] Aik Jun Tan,[1] Pietro Gambardella,[2] and Geoffrey S. D. Beach[1]
[1]*Department of Materials Science and Engineering, Massachusetts Institute of Technology, Cambridge, Massachusetts 02139, USA*
[2]*Department of Materials, ETH Zürich, CH-8093 Zürich, Switzerland*

(Received 26 March 2017; accepted 6 May 2017; published online 18 May 2017)

We report on a memory device concept based on the recently discovered unidirectional spin Hall magnetoresistance (USMR), which can store multiple bits of information in a single ferromagnetic heterostructure. We show that the USMR with possible contribution of Joule heating-driven magnetothermal effects in ferromagnet/normal metal/ferromagnet (FM/NM/FM) trilayers gives rise to four different 2nd harmonic resistance levels corresponding to four magnetization states ($\rightrightarrows$, $\rightleftarrows$, $\leftrightarrows$, $\leftleftarrows$) in which the system can be found. Combined with the possibility of controlling the individual FMs by spin-orbit torques, we propose that it is possible to build an all-electrical lateral two-terminal multi-bit-per-cell memory device. *Published by AIP Publishing.*
[http://dx.doi.org/10.1063/1.4983784]

Beginning with the discoveries of giant magnetoresistance (GMR) and later tunneling magnetoresistance (TMR),[1–4] there has been tremendous effort towards understanding the dynamics of the electron spin and its potential use in electronic circuits, leading to the rapidly developing field of spintronics.[4,5] GMR and TMR provide means for all-electrical readout in magnetic sensors and memory devices based on ferromagnet/spacer/ferromagnet stacks. However, although four distinct stable magnetic states are possible, ($\rightrightarrows$, $\rightleftarrows$, $\leftrightarrows$, $\leftleftarrows$) (arrows indicating the magnetization directions of the two layers), magnetoresistive sensing can only distinguish between two resistance states, parallel and antiparallel. Hence, magnetoresistive stacks require one magnetic layer to remain fixed and serve as a reference layer, rather than to be used to directly store a bit.

The switching of memory cells such as magnetic tunnel junctions has conventionally been accomplished by injecting a spin current from the fixed layer to the free layer or vice-versa to exert spin-transfer torque on the latter. Recently, however, it has been found that spin currents can be more efficiently injected by utilizing the spin Hall effect (SHE)[6] in a nonmagnetic metal (NM) layer adjacent to the ferromagnetic (FM) free layer. An in-plane charge current near the NM/FM interface leads to a vertical spin current that exerts spin-orbit torques (SOTs) that can be used to efficiently control the magnetization.[7–12] This has been used to achieve SOT switching of the free layer in magnetic tunnel junctions,[13–15] efficient current-induced domain wall motion,[16–18] and control of magnetic elements in spin-logic devices.[19]

Recently, the SHE also has been shown to lead to new transport phenomena such as the spin Hall magnetoresistance.[20] A few years later, a related magnetoresistance effect has been reported in NM/FM bilayers, resulting from the interaction of the current-induced interface spin accumulation due to the spin Hall effect and the magnetization.[21–23] This so-called unidirectional spin Hall magnetoresistance (USMR) is a nonlinear and nonreciprocal effect that modulates the longitudinal resistivity depending on the component of the in-plane magnetization vector perpendicular to the current injection direction ($|m_y|$). This allows for the detection of in-plane magnetization reversal along the axis collinear with the interface spin accumulation without requiring an auxiliary magnetic layer, as depicted in Fig. 1(a). Although it is a rather small effect, ~0.002%–0.005% of the total resistance in NM/FM bilayers for a current density of $j = 10^{11}$ A/m^2, the chiral property of the USMR distinguishes it from other linear magnetoresistance effects such as the spin Hall magnetoresistance and anisotropic magnetoresistance, both of which are current-independent and proportional to $|m|^2$. In this letter, we demonstrate experimentally that the USMR can allow for the electrical reading of four

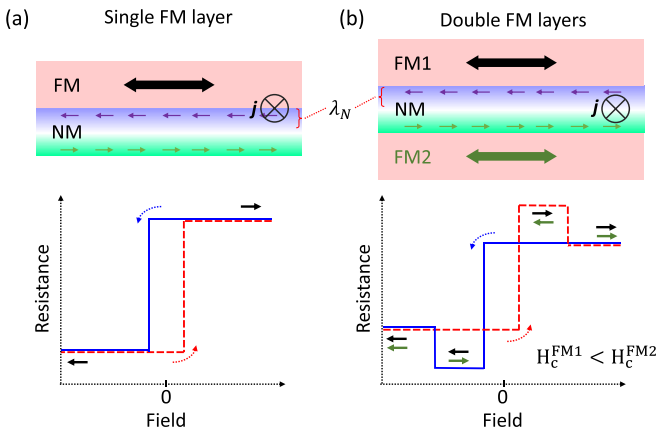

FIG. 1. (a) Illustration of SHE-induced spin accumulation at the interfaces of the normal metal (top) and the change in the longitudinal resistance depending on the magnetization direction collinear with the spin accumulation due to the unidirectional spin hall magnetoresistance (bottom). (b) The effect of adding another ferromagnet to the system with a different coercivity (top). The expected resistance has four levels instead of two, corresponding to the four different magnetic states indicated by the arrows (bottom). λ_N denotes the spin diffusion length of NM.

a)canavci@mit.edu

independent resistance states corresponding to the four distinct magnetic states in a FM/NM/FM stack, allowing us to realize magnetic multi-bit-per-cell memory devices in a straightforward manner.

Thus far, USMR has been reported in bilayer structures where only one interface actively contributes to the effect.[21–24] However, by adding another FM layer in contact with the opposite interface of the NM, it is possible to increase the overall amplitude ($\Delta R/R$) of the effect when the magnetization vectors are aligned antiparallel with respect to each other ($\rightleftarrows$) and to detect the magnetization state of each FM if their coercivities are different ($H_c^{FM1} \neq H_c^{FM2}$). Figure 1(b) shows the proposed structure and the expected USMR signal. The largest (lowest) resistance is obtained when the top magnetization and bottom magnetization are parallel (antiparallel) to the spin accumulation of the respective interfaces. In the ideal case, for the parallel alignment of the two identical FMs, the USMR of the top and bottom interfaces should cancel each other. However, in real devices, differences in the spin transmission and spin current generation may occur due to a slightly different growth mode, strain, and interdiffusion between NMs deposited on FMs and vice versa. Consequently, the interfaces may contribute unevenly to the USMR, as in the case of other spin-orbit-driven effects such as the spin Hall torque[25] and Dzyaloshinskii-Moriya interaction[26] in symmetric Pt/FM/Pt stacks, and produce a net difference between ($\rightrightarrows$) and ($\leftleftarrows$) states. Moreover, the anomalous Nernst (ANE) and spin Seebeck effects (SSE) due to Joule heating and associated temperature gradient perpendicular to the layer plane produce an additional voltage driven by an electric field with symmetry $\mathbf{E} = -\alpha \mathbf{\nabla T} \times \mathbf{m}$, where α is an effective coefficient taking into account both ANE and SSE.[27] In the parallel configuration ($\rightrightarrows$ or $\leftleftarrows$), when $\mathbf{m}$ lies in-plane and perpendicular to the current injection direction, a net difference in the longitudinal voltage should occur between ($\rightrightarrows$) and ($\leftleftarrows$) states. This *magneto-thermal* signal adds to the USMR and can also be effectively used to distinguish between the ($\rightrightarrows$) and ($\leftleftarrows$) states.

Here, we experimentally realize the above FM/NM/FM trilayer structure where we observe four different resistance states similar to Fig. 1(b). We demonstrate that this simple structure can be used as a memory device to store up to four bits of information. Switching between magnetic states is realized by an external magnetic field as low as several tens of Oe. The readout relies on the 2nd harmonic longitudinal resistance measurement, which probes the USMR and magnetothermal voltages and is highly sensitive to the magnetization orientation of each FM layer. We propose that, by further device and material optimization, the writing and reading processes can be used for two-terminal device applications. Furthermore, the writing process can be substituted by SOT and/or Oersted field switching, opening the way to realize lateral two-terminal multi-bit memory devices that can be fully controlled by electrical currents.

We grew Ta(1)/$Co_{50}Fe_{50}$(2)/Pt(3)/$Co_{50}Fe_{50}$(2)/NiO (~12) multilayer stacks [Fig. 2(a)] on a thermally oxidized SiO_2 substrate by DC magnetron sputtering. Here, thicknesses are in nm and subscripts denote at. %. The Ta underlayer serves as a buffer layer and is expected to be highly resistive, and thus its contribution to the conduction can be neglected. The NiO layer is grown reactively by sputtering Ni in the presence of a partial pressure of ≈1.5 mTorr of O_2. Its role is to enhance the coercivity of the top CoFe layer with respect to the bottom one.[28] Depositions were performed in an in-plane field of ~100 Oe to induce a uniaxial in-plane magnetic anisotropy in the CoFe layers.

We characterized the magnetic properties of the continuous multilayer stack by vibrating sample magnetometry. Figure 2(b) shows the representative easy axis (red curve) and hard axis (black curve) hysteresis loops for the CoFe/Pt/CoFe/NiO film. By considering the total CoFe thickness of 4 nm, we find the saturation magnetization value of $1.7 \pm 0.1 \times 10^6$ A/m, which is slightly below the bulk value of CoFe (~1.95×10^6 A/m). The hard-axis loop is sheared, while the easy-axis loop exhibits two distinct steps corresponding to switching of the two CoFe layers. Note that in addition to enhancing the coercivity, the NiO layer induces a small exchange bias, resulting in a loop shift along the field axis.

To perform the electrical measurements, we fabricated Hall bar devices using standard optical lithography and lift-off. The deposition for Hall bars was performed simultaneously with the continuous layers discussed above, and thus, their properties are expected to be very similar. The device structure, coordinates, and measurement scheme are depicted in Fig. 2(c). To probe the USMR and magnetothermal effects, we measured the longitudinal 2nd harmonic voltage ($V_{2\omega}$) using a standard lock-in method with an ac density of $j_{rms} \sim 10^{10}$ A/m^2 and a frequency of 1916 Hz and with field H_{ext} swept along the y-axis. To improve the signal-to-noise ratio at the low probing current densities used, data were averaged over ~100 field sweep cycles. All measurements were performed at room temperature.

Figure 3(a) shows $V_{2\omega}$ versus H_y for CoFe/Pt/CoFe, with $j_{rms} = 1.16 \times 10^{10}$ A/m^2. The sample exhibits four distinct $V_{2\omega}$ signal levels corresponding to four different magnetization states ($\rightrightarrows$, $\leftleftarrows$, $\rightleftarrows$, $\leftrightarrows$). The data closely resembles the behavior expected from the USMR and magnetothermal effects as shown in Fig. 1(b). There is a large difference in $V_{2\omega}$ between the two antiparallel states ($\rightleftarrows$, $\leftrightarrows$), where the USMR, ΔR_{usmr}, is expected to be maximum and the

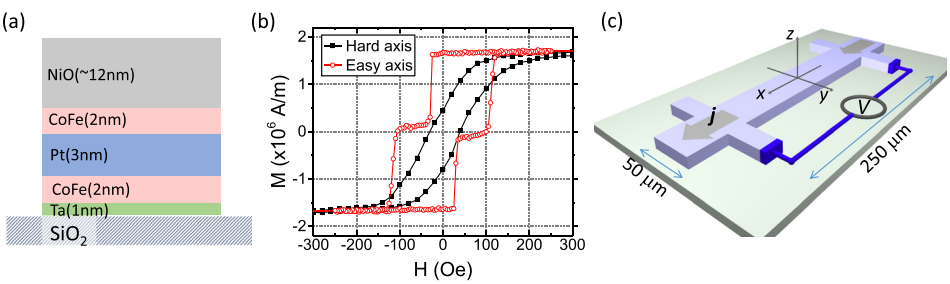

FIG. 2. (a) Layer structure and (b) magnetization curves of CoFe/Pt/CoFe layers obtained by vibrating sample magnetometry. Two step reversal along the easy axis shows that the top and bottom CoFe layers switch at different fields. (c) Device structure, coordinate axis, and measurement scheme.

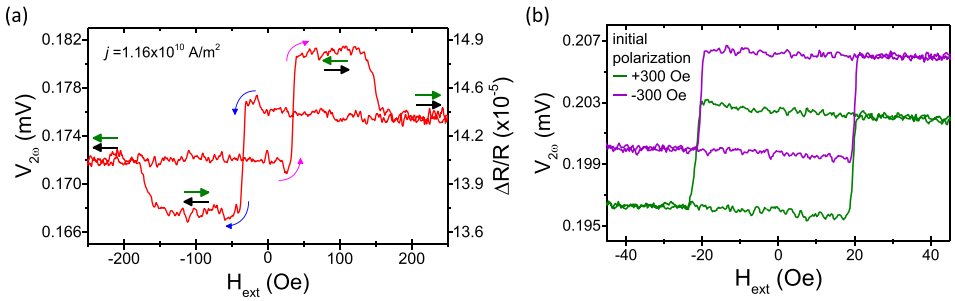

FIG. 3. (a) Voltage difference corresponding to the four different magnetic states of CoFe/Pt/CoFe multilayers measured during a field sweep along the y-axis. (b) Minor loops measured after initial polarization of the top CoFe layer with ±300 Oe. Depending on the magnetization orientation of the top CoFe layer, the overall signal shifts vertically, demonstrating that it is possible to obtain four stable signal levels at a zero field.

magnetothermal effect to vanish by symmetry. The extrapolation of the data to $j = 10^{11}$ A/m^2 (for a comparison with the literature) yields $\Delta R/R \cong 7 \times 10^{-5}$, which is more than twice larger with respect to the Pt(3)/Co(2.5) bilayer studied in Ref. 21, and represents the largest USMR effect obtained so far in all-metallic layers. However, we caution that, even in the antiparallel configuration, a non-zero magnetothermal effect might be present if ∇T experienced by each FM layer is different. For instance, based on previous work,[27] there is a possibility that the bottom CoFe layer, being closer to the substrate, experiences a larger temperature gradient and produces a higher magnetothermal signal with respect to the top CoFe layer. Thereby, the USMR contribution might be lower or higher than this value depending on the difference in the thermal gradients across the two FM layers. Unfortunately, standard methods to quantitatively separate magnetothermal, spin-orbit torque, and USMR signals cannot be easily used in this double FM layers, and therefore, we are unable to quantify the exact value of the USMR.

In order to demonstrate the independent programming of the four $V_{2\omega}$ states, we perform an experiment where we initially configure the top layer by applying a large field (in excess of its larger coercivity H_c) and then switch the bottom layer by cycling through a minor loop. Figure 3(b) shows such measurements for the CoFe/Pt/CoFe layer. Prior to measurements, a field of +300 Oe or −300 Oe was applied to set the top CoFe magnetization direction. Then, the field was swept between ±45 Oe. We note that the curves shift vertically depending on the orientation of the top CoFe layer, allowing us to obtain four different signal levels at a zero external field.

Finally, we demonstrate the selective switching between different magnetic configurations using tailored field pulse sequences and subsequent electrical readout of those states. The measurements are described in Fig. 4. The upper and lower panels show the field input and the signal output, respectively, in the absence of the field. Here, a field larger than 200 Oe is used to set the top layer, followed by a field magnitude of 30 Oe that sets the bottom layer orientation.

We remark that the signal levels in this device, while sufficient to distinguish the four states, can be significantly optimized further. For instance, injecting a larger current will increase the $V_{2\omega}$ output. Since $V_{2\omega}$ scales with I^2, increasing the applied current tenfold, i.e., to the $\sim 10^{11}$ A/m^2 range, will result in an enhancement of two orders of magnitude in $V_{2\omega}$. The optimization of the layer thicknesses, FM choice, and device design could increase the output voltage even further. Another possibility is to use other spin-orbit materials instead of conventional heavy metals. For instance, using semiconductors and topological insulators with large charge-spin conversion could substantially boost the USMR signals.[23,24]

Finally, we remark that inasmuch as the device involves NM/FM layers in which strong spin-orbit torques are expected, it should be straightforward to design in-plane current-switched multi-bit memory elements rather than devices switched by the field.[8,13,19] Moreover, while here we consider stacks with two FM layers, the concept can be readily scaled to higher bit densities by including additional layers in the stack. By combining NMs with opposite spin Hall angles and FMs with different H_c values, such as a device comprising FM_1/Pt/FM_2/Ta/FM_3, one could realize 8 different magnetization states each with a unique $V_{2\omega}$ signal.

In conclusion, we have demonstrated that in a trilayer structure consisting of FM/NM/FM, it is possible to enhance the amplitude of the USMR by including an additional FM/NM interface and to detect the in-plane magnetization direction of each FM perpendicular to the current injection. The detection relies on the 2nd harmonic resistance measurements driven by the USMR with possible contribution of Joule heating-induced magnetothermal effects (ANE and SSE). The four different magnetization states give rise to four unique resistance levels, which can be read out by a simple two-terminal electric measurement. We propose that by further optimization, it is possible to build a lateral two-terminal

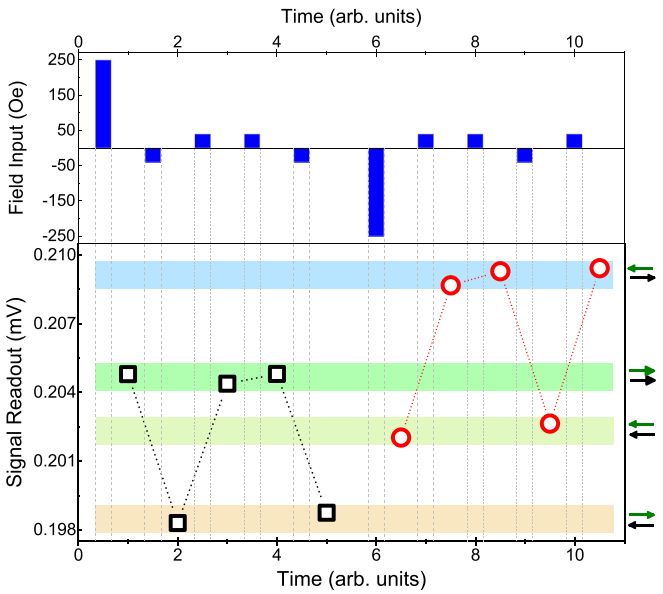

FIG. 4. Demonstration of the four-state USMR device. Depending on the input field, it is possible to set the system in one of the four states and read the state with the longitudinal $V_{2\omega}$ measurements. The top plot shows the field pulse sequence, and the bottom one shows $V_{2\omega}$ measured after the pulse.

device that can store multiple magnetic bits. Moreover, the magnetic states can be manipulated by spin-orbit torques, thereby opening the possibility for all-electrical operation.

This work was supported by C-SPIN, one of the six SRC STARnet Centers, sponsored by MARCO (USA) and DARPA (USA).

[1]M. N. Baibich, J. M. Broto, A. Fert, F. Nguyen Van Dau, F. Petroff, P. Etienne, G. Creuzet, A. Friederich, and J. Chazelas, Phys. Rev. Lett. **61**, 2472 (1988).
[2]G. Binasch, P. Grünberg, F. Saurenbach, and W. Zinn, Phys. Rev. B **39**, 4828(R) (1989).
[3]S. Yuasa, T. Nagahama, A. Fukushima, Y. Suzuki, and K. Ando, Nat. Mater. **3**, 868 (2004).
[4]C. Chappert, A. Fert, and F. N. Van Dau, Nat. Mater. **6**, 813 (2007).
[5]I. Žutić, J. Fabian, and S. Das Sarma, Rev. Mod. Phys. **76**, 323 (2004).
[6]J. Sinova, S. O. Valenzuela, J. Wunderlich, C. H. Back, and T. Jungwirth, Rev. Mod. Phys. **87**, 1213 (2015).
[7]I. M. Miron, K. Garello, G. Gaudin, P.-J. Zermatten, M. V. Costache, S. Auffret, S. Bandiera, B. Rodmacq, A. Schuhl, and P. Gambardella, Nature **476**, 189 (2011).
[8]L. Liu, C.-F. Pai, Y. Li, H. W. Tseng, D. C. Ralph, and R. A. Buhrman, Science (80-). **336**, 555 (2012).
[9]K. Garello, I. M. Miron, C. O. Avci, F. Freimuth, Y. Mokrousov, S. Blügel, S. Auffret, O. Boulle, G. Gaudin, and P. Gambardella, Nat. Nanotechnol. **8**, 587 (2013).
[10]J. Kim, J. Sinha, M. Hayashi, M. Yamanouchi, S. Fukami, T. Suzuki, S. Mitani, and H. Ohno, Nat. Mater. **12**, 240 (2013).
[11]X. Fan, H. Celik, J. Wu, C. Ni, K. Lee, V. O. Lorenz, and J. Q. Xiao, Nat. Commun. **5**, 3042 (2014).
[12]C. O. Avci, A. Quindeau, C.-F. Pai, M. Mann, L. Caretta, A. S. Tang, M. C. Onbasli, C. A. Ross, and G. S. D. Beach, Nat. Mater. **16**, 309 (2017).
[13]C.-F. Pai, L. Liu, Y. Li, H. W. Tseng, D. C. Ralph, and R. A. Buhrman, Appl. Phys. Lett. **101**, 122404 (2012).
[14]M. Cubukcu, O. Boulle, M. Drouard, K. Garello, C. O. Avci, I. M. Miron, J. Langer, B. Ocker, P. Gambardella, and G. Gaudin, Appl. Phys. Lett. **104**, 42406 (2014).
[15]M. Yamanouchi, L. Chen, J. Kim, M. Hayashi, H. Sato, S. Fukami, S. Ikeda, F. Matsukura, and H. Ohno, Appl. Phys. Lett. **102**, 212408 (2013).
[16]P. P. J. Haazen, E. Murè, J. H. Franken, R. Lavrijsen, H. J. M. Swagten, and B. Koopmans, Nat. Mater. **12**, 299 (2013).
[17]S. Emori, U. Bauer, S.-M. Ahn, E. Martinez, and G. S. D. Beach, Nat. Mater. **12**, 611 (2013).
[18]K. Ryu, L. Thomas, S. Yang, and S. Parkin, Nat. Nanotechnol. **8**, 527 (2013).
[19]D. Bhowmik, L. You, and S. Salahuddin, Nat. Nanotechnol. **9**, 59 (2013).
[20]H. Nakayama, M. Althammer, Y. T. Chen, K. Uchida, Y. Kajiwara, D. Kikuchi, T. Ohtani, S. Geprägs, M. Opel, S. Takahashi, R. Gross, G. E. W. Bauer, S. T. B. Goennenwein, and E. Saitoh, Phys. Rev. Lett. **110**, 206601 (2013).
[21]C. O. Avci, K. Garello, A. Ghosh, M. Gabureac, S. F. Alvarado, and P. Gambardella, Nat. Phys. **11**, 570 (2015).
[22]C. O. Avci, K. Garello, J. Mendil, A. Ghosh, N. Blasakis, M. Gabureac, M. Trassin, M. Fiebig, and P. Gambardella, Appl. Phys. Lett. **107**, 192405 (2015).
[23]K. Olejnik, V. Novák, J. Wunderlich, and T. Jungwirth, Phys. Rev. B **91**, 180402 (2015).
[24]K. Yasuda, A. Tsukazaki, R. Yoshimi, K. S. Takahashi, M. Kawasaki, and Y. Tokura, Phys. Rev. Lett. **117**, 127202 (2016).
[25]M. Yang, K. Cai, H. Ju, K. W. Edmonds, G. Yang, and S. Liu, Sci. Rep. **6**, 20778 (2016).
[26]R. Lavrijsen, D. M. F. Hartmann, A. Van Den Brink, Y. Yin, B. Barcones, R. A. Duine, M. A. Verheijen, H. J. M. Swagten, and B. Koopmans, Phys. Rev. B **91**, 104414 (2015).
[27]C. O. Avci, K. Garello, M. Gabureac, A. Ghosh, A. Fuhrer, S. F. Alvarado, and P. Gambardella, Phys. Rev. B **90**, 224427 (2014).
[28]J. Nogues and I. K. Schuller, J. Magn. Magn. Mater. **192**, 203 (1999).